Neurobiology of Stress 32 (2024) 100666

Contents lists available at ScienceDirect

Neurobiology of Stress

journal homepage: www.elsevier.com/locate/ynstr

DCC, a potential target for controlling fear memory extinction and hippocampal LTP in male mice receiving single prolonged stress

Shaojie Yang [a,1], Jiamin Hu [b,1], Yuzhuang Chen [b,1], Zhengrong Zhang [b], Jingji Wang [a], Guoqi Zhu [b,*]

[a] Acupuncture and Moxibustion Clinical Medical Research Center of Anhui Province, The Second Affiliation Hospital of Anhui University of Chinese Medicine, Shouchun Road 300, Hefei, 230061, China

[b] Center for Xin'an Medicine and Modernization of Traditional Chinese Medicine of IHM, and Key Laboratory of Molecular Biology (Brain diseases), Anhui University of Chinese Medicine, Longzhihu Road 350, Hefei, 230012, China

ARTICLE INFO

Keywords:
Post-traumatic stress disorder
DCC
Fear memory
LTP
Hippocampus

ABSTRACT

Post-traumatic stress disorder (PTSD) is a severe stress-dependent psychiatric disorder characterized by impairment of fear memory extinction; however, biological markers to determine impaired fear memory extinction in PTSD remain unclear. In male mice with PTSD-like behaviors elicited by single prolonged stress (SPS), 19 differentially expressed proteins in the hippocampus were identified compared with controls. Among them, a biological macromolecular protein named deleted in colorectal cancer (DCC) was highly upregulated. Specific overexpression of DCC in the hippocampus induced similar impairment of long-term potentiation (LTP) and fear memory extinction as observed in SPS mice. The impairment of fear memory extinction in SPS mice was improved by inhibiting the function of hippocampal DCC using a neutralizing antibody. Mechanistic studies have shown that knocking down or inhibiting μ-calpain in hippocampal neurons increased DCC expression and induced impairment of fear memory extinction. Additionally, SPS-triggered impairment of hippocampal LTP and fear memory extinction could be rescued through activation of the Rac1–Pak1 signaling pathway. Our study provides evidence that calpain-mediated regulation of DCC controls hippocampal LTP and fear memory extinction in SPS mice, which likely through activation of the Rac1–Pak1 signaling pathway.

1. Introduction

Post-traumatic stress disorder (PTSD) is a serious psychiatric illness triggered by catastrophic or stressful events. Fear memory abnormalities, trauma stimulation avoidance, increased alertness, anxiety, and irritability are the core symptoms of PTSD. A study published in the *Lancet* reported that the prevalence of PTSD was 15.3% in people living in conflict area settings (Charlson et al., 2019). Clinical and experimental studies agree that impairment of fear memory extinction is the core feature of PTSD (Richter-Levin et al., 2018; Stein et al., 2021). The hippocampus plays a critical role in the acquisition and storage of contextual fear memory (Hallock et al., 2020; Oh and Han, 2020). Furthermore, neurons may weaken the existing fear memory in the hippocampus through remodeling, promoting removal of the fear memory. This is thought to be the basic principle of exposure therapy for PTSD (Frankland and Josselyn, 2016). Therefore, exploring the key targets related to the fear memory extinction in the hippocampus is of great significance for the treatment of PTSD.

Deleted in colorectal cancer (DCC) is a single transmembrane protein consisting of a signal peptide motif and 11 domains, including multiple immunoglobulin-like domains, a transmembrane domain, and several fibronectin type 3 domains. As a netrin-1 receptor, the role of DCC has been extensively investigated in axonal growth and development (Mehlen and Mazelin, 2003; Morcom et al., 2021; Robinson et al., 2021; Zang et al., 2022). However, DCC expression in the brain tends to decrease during adulthood (Osborne et al., 2005). Thus, abnormal DCC expression might be harmful for the mental or emotional health of adults. A genome-wide association study (GWAS) analysis suggests that the *DCC* gene is associated with emotional instability, which can lead to depression and other mental disorders (Ward et al., 2017). However, whether and how DCC participates in the occurrence of PTSD has not

* Corresponding author.
E-mail addresses: shaojieyang20@hotmail.com (S. Yang), 2437204706@qq.com (J. Hu), chen_yuzhuang@126.com (Y. Chen), zrzhang311@126.com (Z. Zhang), wangjingji@ahtcm.edu.cn (J. Wang), guoqizhu@gmail.com (G. Zhu).

[1] Shaojie Yang, Jiamin Hu and Yuzhuang Chen contributed equally to this work.

https://doi.org/10.1016/j.ynstr.2024.100666
Received 13 April 2024; Received in revised form 29 June 2024; Accepted 6 August 2024
Available online 8 August 2024

Abbreviations

PTSD	post-traumatic stress disorder
DCC	deleted in colorectal cancer
SPS	single prolonged stress
GWAS	genome-wide association study
NMDAR	N-methyl-D-aspartate receptor
LTP	long-term potentiation
PFC	prefrontal cortex
LTD	long-term depression

been directly reported. The RAS-related C3 botulinum toxin substrate 1 (RAC1)–P21-activated kinase 1 (PAK1) pathway is a crucial signaling cascade involved in various biological processes, including cytoskeletal reorganization, cell migration, proliferation, survival, and synaptic plasticity (Zhang et al., 2021). Activity-regulated cytoskeleton-associated protein (ARC) is a protein that plays a pivotal role in synaptic plasticity; its expression and regulation are closely linked to learning and memory. The absence of ARC can result in memory deficits, making it an important marker for assessing synaptic function (Chen et al., 2023). Interestingly, DCC can mediate netrin-1 signaling to activate downstream RAC1, thereby regulating actin membrane extension and influencing cell motility (Shekarabi and Kennedy, 2002). Therefore, we hypothesize that DCC may contribute to the onset of PTSD through the RAC1–PAK1 pathway.

In this study, we delivered single prolonged stress (SPS) in male mice to explore the mechanism underlying impaired fear memory extinction in PTSD. Initially, we screened the SPS-induced differentially expressed proteins (DEPs) in the hippocampus. Second, based on the results of the proteomics, we further confirmed the critical function of DCC in the impairment of fear memory extinction in SPS mice. Finally, mechanistic studies were performed to determine the causation of hippocampal DCC upregulation. The results of this study will provide new insights into the pathogenesis of PTSD, prompting future drug development studies.

2. Materials and methods

2.1. Animals and modeling

Male C57BL/6 mice (3 months old, 20–25 g) were purchased from Hangzhou Ziyuan Experimental Animal Technology Co., Ltd (production license number: SCXK (Zhe) 2019-0004). The animal feeding conditions were as follows: temperature of 22 ± 2 °C, relative humidity 45–65%, a 12 h light/12 h dark cycle, and water and food ad libitum. After 7 days of adaptation, the SPS model was replicated according to the method described in previous publications (Feng et al., 2020; Gao et al., 2023). In brief, the mice were subjected to forced swim stress for 20 min following 2 h of restraint. After a 15 min rest, the mice were anesthetized with 5% isoflurane. Upon regaining consciousness, the mice were placed in a shock box and administered a single foot shock (2 mA, 2 s) without a conditioned context. The Control group underwent food and water deprivation during the SPS modeling period. The animal modeling and treatment procedure of this study was approved by the Experimental Animal Ethics Committee of Anhui University of Chinese Medicine (Animal Ethics No.: AHUCM-mouse-2022014).

2.2. Animal groups and experimental procedures

Experiment 1: After 7 days of adaptation, mice were randomly divided into the Control group and SPS group. The mice in SPS group received the SPS regime. After 14 days, the hippocampal tissues of the two groups underwent proteomic differential protein analysis (n = 6 per group). In a separate experiment, after 14 days, behavioral tests (described below) were performed for the Control and SPS group (n = 6, per group). Following the behavioral tests, the hippocampus was extracted, and western blotting and immunofluorescence staining were conducted. In addition, the dynamic detection of DCC in the hippocampus of SPS mice was divided into four time points: day 0 (D0), day 1 (D1), day 7 (D7), and day 14 (D14), and the expression level of DCC was detected by western blotting (n = 5 per group) (Fig. 1A).

Experiment 2: Mice were randomly divided into the Scramble group, Scramble + SPS group, overexpression DCC (OE-DCC) group, and OE-DCC + SPS group (n = 11 per group). The designed control null-loaded virus LV-CaMKIIa- 3xFlag-WPRE (BrainVTA Co., Ltd.) was injected into the bilateral hippocampal CA1 regions (bregma: 2.3 mm, LR: ±2.0 mm, H: 1.55 mm) of mice in scramble group and Scramble + SPS group. A DCC overexpression virus LV-CaMKIIa- DCC-3xFlag-WPRE (BrainVTA Co., Ltd.) was injected into the bilateral hippocampal CA1 regions of mice in the OE-DCC group and OE-DCC + SPS group at the same coordinate position. The injection volume of both viruses was 500 nL/side. After 14 days of virus expression, the Scramble + SPS group and OE-DCC + SPS group were treated with the SPS paradigm. On day 28, behavioral tests were performed. In addition, to ascertain whether the upregulation of DCC was responsible for the disruption of long-term potentiation (LTP), electrophysiological experiments were conducted to examine the changes in LTP in Schaffer collateral-CA1 synapses in both the Scramble and OE-DCC mice. Additionally, the expression of DCC was confirmed by western blotting (Fig. 2A).

Experiment 3: Mice were randomly divided into the Control + Anti-DCC(−) group, SPS + Anti-DCC(−) group, Control + Anti-DCC(+) group, and SPS + Anti-DCC(+) group (n = 6 in each group). We modified the method reported in the reference with the addition of a pre-experimental neutralizing antibody to determine this research scheme (Lu et al., 2022). On day 11, mice in the Control + Anti-DCC(+) group and SPS + Anti-DCC(+) group were injected with a mouse-derived DCC monoclonal antibody (sc-515834, Santa Cruz Biotechnology) into the CA1 area (bregma: 2.3 mm, LR: ±2.0 mm, H: 1.50–1.65 mm) on both sides of the hippocampus (1.5 μL/side). The mice in the Control + Anti-DCC(−) group and SPS + Anti-DCC(−) group were injected with the same amount of DCC inactivated antibody at the same location. On day 14, the behavior of the mice in each group was tested (Fig. 3A).

Experiment 4: After 7 days of adaptation, the mice were randomly divided into the Scramble group, μ-calpain knockdown (KD) group, and μ-calpain KD + SPS group (n = 4 in each group). The designed control null-loaded virus rAAV-CMV- (EGFP-U6)-shRNA(scramble)-WPRE-pA (BrainVTA Co., Ltd.) was localized and injected into the hippocampus of Scramble mice. The injection location and virus injection volume were consistent with our previous report (Gao et al., 2023). μ-calpain KD virus rAAV-CMV-(EGFP-U6)-shRNA(μ-calpain)-WPRE-pA was localized and injected into the hippocampus of mice in the μ-calpain KD group and μ-calpain KD + SPS group using the same method. After 28 days, the SPS model was replicated in the μ-calpain KD + SPS group. After 14 days of modeling, hippocampal tissue was taken for western blotting analysis (**S 1A**).

Experiment 5: Mice were randomly divided into the Control group, SPS group, Control + Calpeptin group, and SPS + Calpeptin group (n = 7 in each group). Mice in the SPS + Calpeptin group and Control + Calpeptin group were injected intraperitoneally with calpeptin (2.0 mg/kg, ≥98%, SJ-MX0984, Sparkjade). The dose of calpeptin was selected based on our previous publication, in which we showed that hippocampal calpain activity was inhibited by this dose (Song et al., 2020). Mice in the Control group and SPS group were injected with the same amount of saline. Intraperitoneal injection was administered once a day for 14 days. After 14 days, the behavior of the mice in each group was tested. At the end of the behavioral tests, hippocampal tissue was taken for western blotting analysis (Fig. 4A).

Experiment 6: Mice were randomly divided into the Control group, SPS group, and SPS + NSC23766 group (n = 10 in each group). The SPS + NSC23766 group were injected intraperitoneally with the RAC1

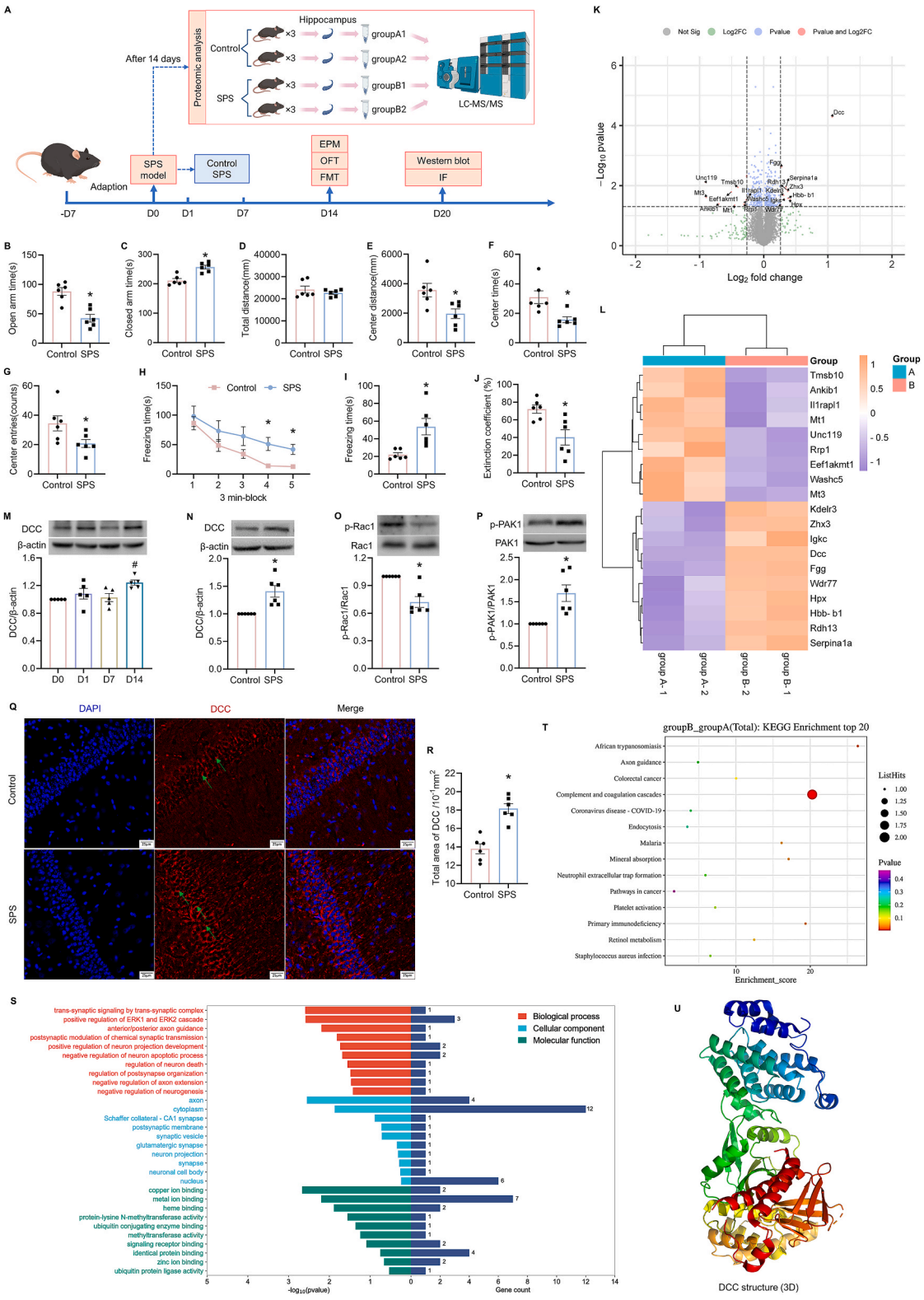

Fig. 1. The expression of DCC and Rac1-PAK1 signaling pathway is abnormal in the hippocampus of SPS mice. (A) Experiment 1 protocol; (B–C) Open arm time and closed arm time of EPM (n = 6); (D–G) Total distance, center distance, center time and center entries of OFT (n = 6); (H–J) The freezing time of FMT in re-exposure period and extinction period, and extinction coefficient (n = 6); (K) Volcanic diagram of total protein count and its increase and decrease in SPS group and Control group; (L) Heat map of differential proteins in the SPS group and Control group; (M) DCC protein levels in D0, D1, D7 and D14 during SPS modeling (n = 5); (N–P) DCC, p-Rac1 and p-PAK1 protein levels in Control group and SPS group (n = 3, repeat twice); (Q–R) Immunofluorescence images of DCC protein and the number of DCC puncta and the total area of DCC puncta (n = 3, repeat twice); (S) GO analysis of total differential protein; (T) KEGG analysis of total differential protein; (U) 3D structure of DCC. Data were expressed as means ± SEM. $^{\#}p < 0.05$ *vs.* D0 (One-way ANOVA), $^{*}p < 0.05$ *vs.* the Control group (Tukey's test or *t*-test).

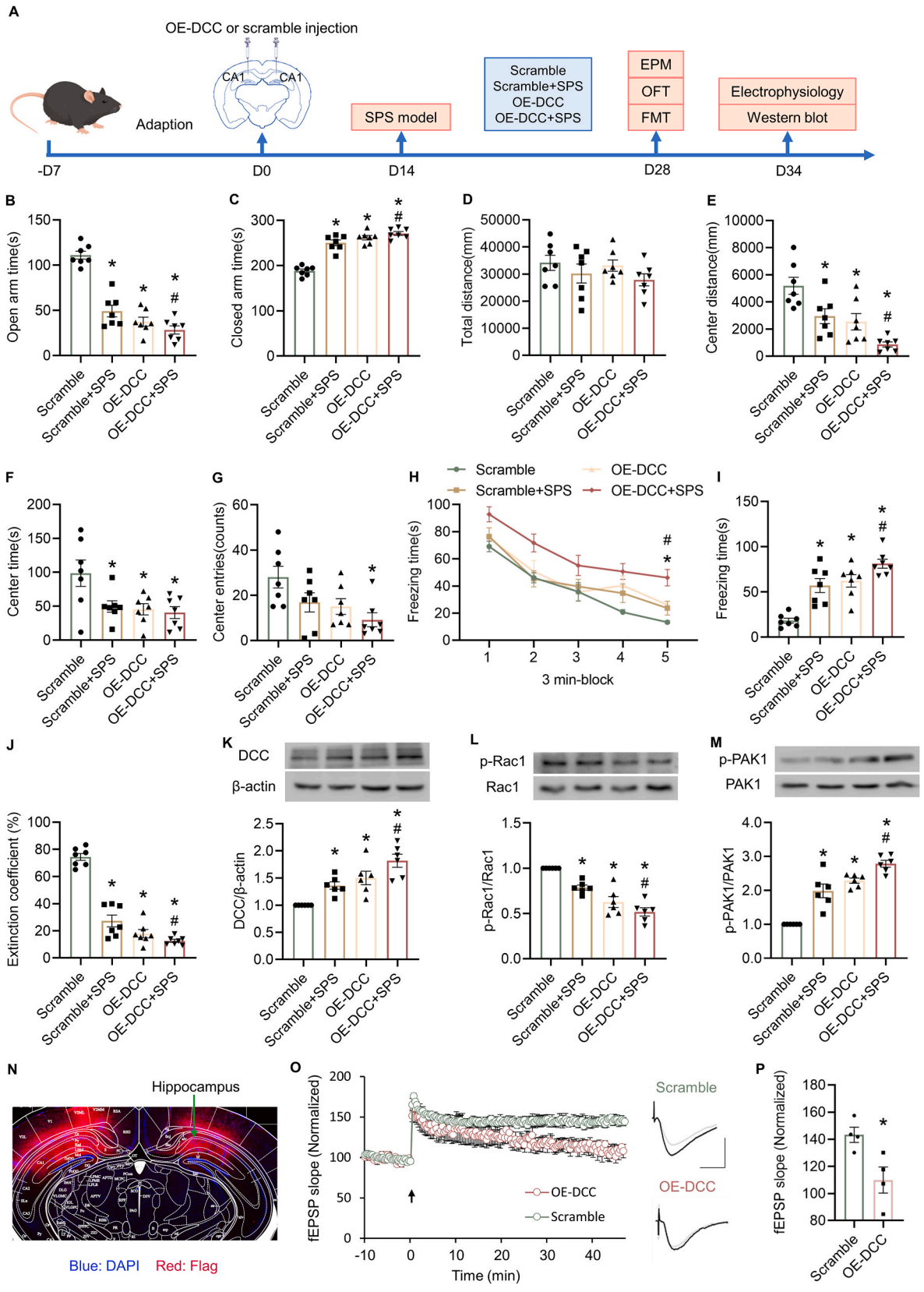

Fig. 2. Overexpression of DCC impairs fear memory extinction and hippocampal LTP. (A) Experiment 2 protocol; (B–C) Open arm time and closed arm time of EPM (n = 7); (D–G) Total distance, center distance, center time and center entries of OFT (n = 7); (H–J) The freezing time of FMT in extinction session and after extinction, and extinction coefficient (n = 7); (K–M) Western blot analysis of protein expression of DCC, p-Rac1 and p-PAK1 (n = 3, repeat twice); (N) Immunofluorescence was used to verify the localized injection of virus in hippocampal CA1 region of mice; (O–P) LTP analysis and comparison of the results at the 40th min after TBS (indicated by arrow) (n = 4). The insertions were the traces of the baseline and the 40th min time points (0.5 mV/10 ms). Data were expressed as means ± SEM. $^{*}p < 0.05$ *vs.* the Scramble group, $^{\#}p < 0.05$ *vs.* the Scramble + SPS group (Tukey's test or *t*-test).

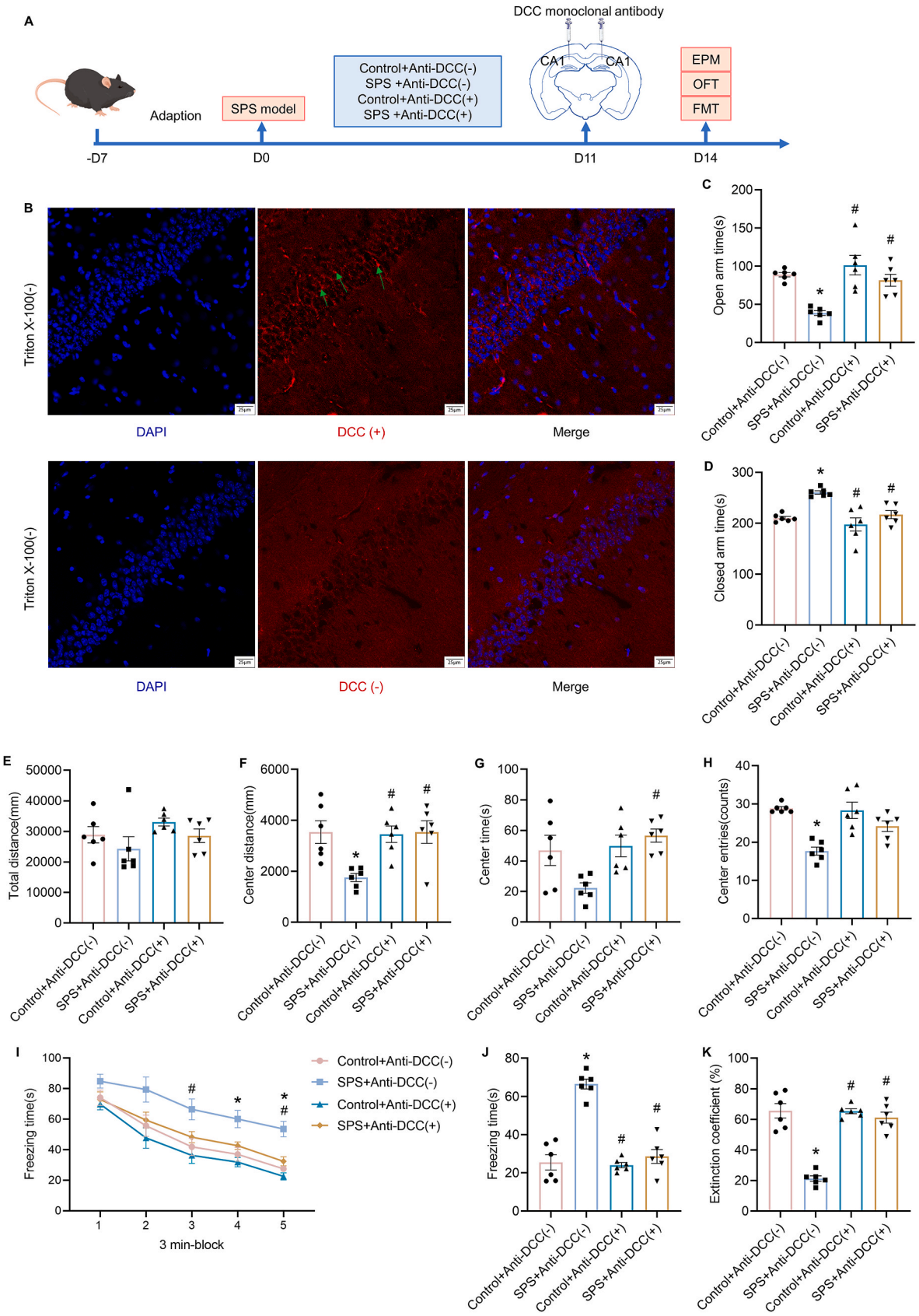

Fig. 3. Impairment of fear memory extinction in SPS mice is improved by neutralizing DCC function. (A) Experiment 3 protocol; (B) Without the use of Triton X-100 to permeate the cell membrane, DCC antibody could still bind to DCC on the membrane; (C–D) Open arm time and closed arm time of EPM (n = 6); (E–H) Total distance, center distance, center time and center entries of OFT (n = 6); (I–K) The freezing time of FMT in re-exposure period and extinction period, and extinction coefficient (n = 6). Data were expressed as means ± SEM. $^{*}p < 0.05$ *vs.* the Control + Anti-DCC(−) group, $^{\#}p < 0.05$ *vs.* the SPS + Anti-DCC(−) group (Tukey's test or Dunn's test).

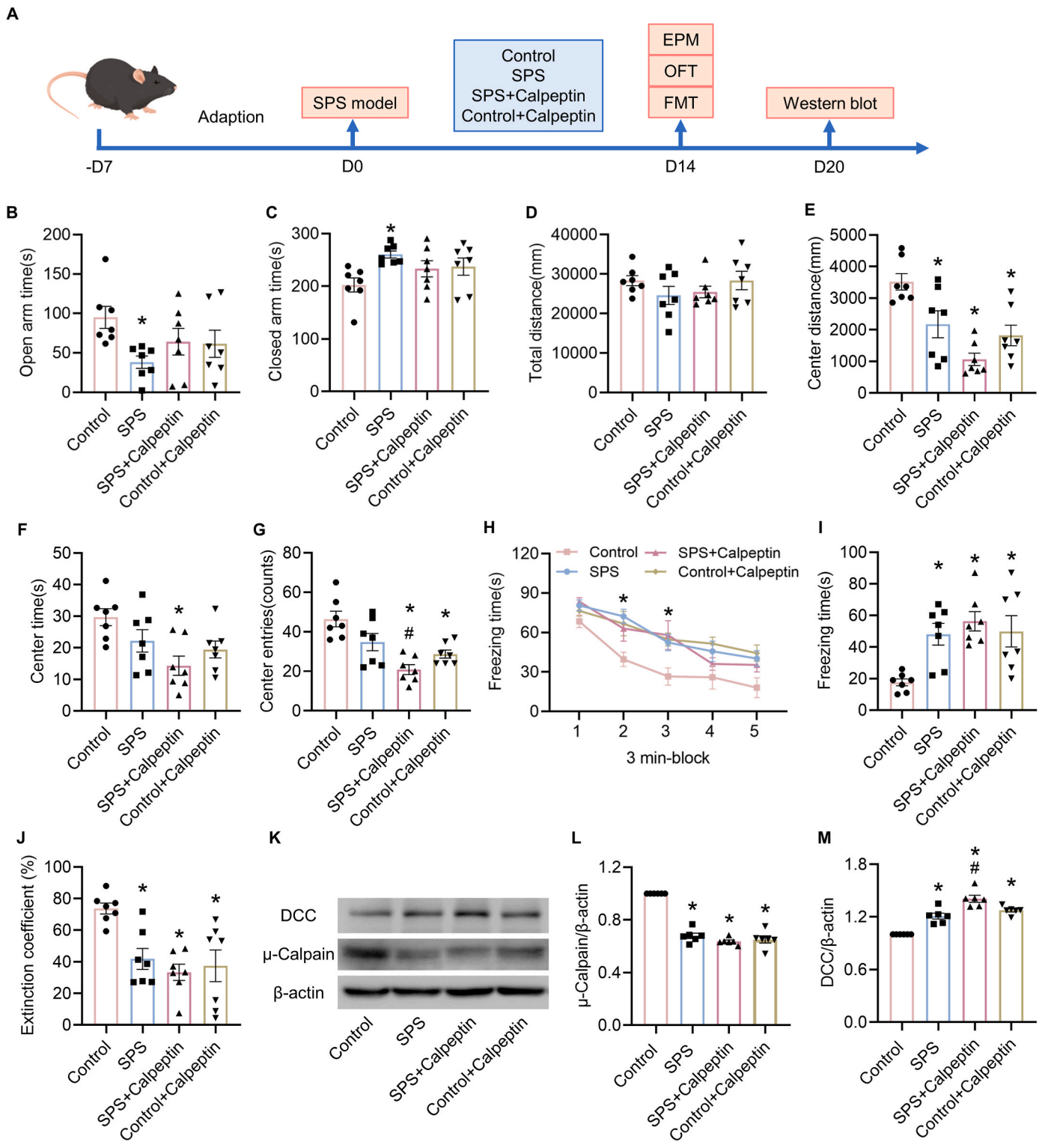

Fig. 4. Chronic administration of calpeptin promotes induces impairment of fear memory extinction. (A) Experiment 5 protocol; (B–C) Open arm time and closed arm time of EPM (n = 7); (D–G) Total distance, center distance, center time and center entries of OFT (n = 7); (H–J) The freezing time of FMT in re-exposure period and extinction period, and extinction coefficient (n = 7); (K) Representative western blots of DCC, μ-Calpain and β-actin; (L–M) Quantitative data for μ-Calpain and DCC (n = 3, repeat twice). Data are expressed as means ± SEM. $^{*}p < 0.05$ vs. the Control group, $^{\#}p < 0.05$ vs. the SPS group (Tukey's test or Dunn's test).

inhibitor NSC23766 (2.5 mg/kg, ≥97%, S8031, Selleck). The dose of NSC23766 was selected based on a previous reference (Sha et al., 2022). Mice in the Control group and SPS group were injected with the same amount of normal saline. Intraperitoneal injection was administered once a day for 14 days. After 14 days, behavioral tests were executed. At the end of the behavioral tests, hippocampal tissue was taken for electrophysiological experiments, western blotting, and immunofluorescence staining (Fig. 5A).

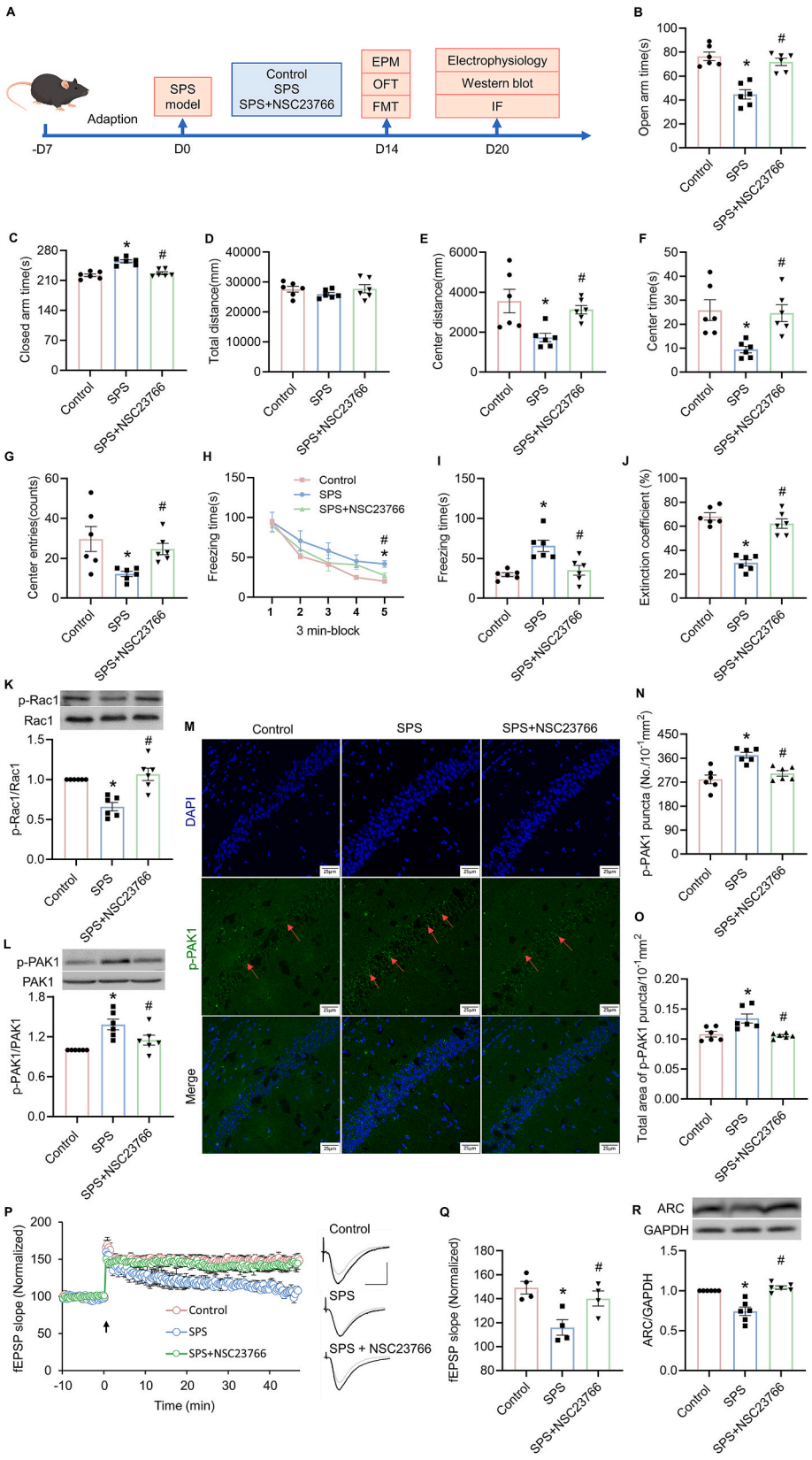

Fig. 5. NSC23766 improves the fear memory extinction and anxiety-like behavior, and inhibits the activation of the Rac1-PAK1 signaling pathway in the hippocampus of SPS mice. (A) Experiment 6 protocol; (B–C) Open arm time and closed arm time of EPM (n = 6); (D–G) Total distance, center distance, center time and center entries of OFT (n = 6); (H–J) The freezing time of FMT in re-exposure period and extinction period, and extinction coefficient (n = 6); (K–L) Western blot analysis of protein expression of p-Rac1 and p-PAK1 (n = 3, repeat twice); (M–O) Immunofluorescence images of p-PAK1 protein and the number of p-PAK1 puncta and the total area of p-PAK1 puncta (n = 3, repeat twice); (P–Q) LTP analysis and comparison of the results at the 40th min time point (n = 4). The insertions were

the traces of the baseline and 40th min time points (0.5 mV/10 ms); (R) Western blot analysis of protein expression of ARC (n = 3, repeat twice). Data are expressed as means ± SEM. *$p < 0.05$ *vs.* the Control group, #$p < 0.05$ *vs.* the SPS group (Tukey's test or Dunn's test).

2.3. Behavioral tests

The time table of behavioral tests included the following: open field test (OFT) (D1), elevated plus maze test (EPM) (D2), and the fear memory test (FMT) (D3–6). Each behavioral experiment was conducted with a 24 h interval. Similarly, the four periods of the FMT were spaced with 24 h intervals. The specific protocols for each behavioral test are detailed below.

OFT: The mice were adapted to the environment before the test. During the test, the mice were placed in the central area of the open field device. The Super Maze software was used to record the total distance, center distance, center time, and center entries in 5 min.

EPM: The mice were adapted to the environment before the test. During the test, the mice were placed in the direction of the open arm in the central area of the elevated plus maze. The time spent in the open and closed arms in the elevated plus maze in 5 min was recorded using Super Maze software (Shanghai Xinruan Information Technology).

FMT: The experiment on the extinction of fear memory is divided into four phases: an adaptation period, a training period, a re-exposure period, and an extinction period with a 24 h interval between each. D1 was the adaptation period; mice were kept in the fear box (UgoBasile, Gemonio, Italy) for 5 min without foot shock. D2 was the training period; mice were kept in the fear box for 5 min and were given three-foot shocks (1.0 mA, 2 s, at 73–74 s intervals). D3 was the re-exposure period; mice were kept in the fear box without foot shock for 15 min. Each 3 min was set as a unit, and the ANY-Maze software was used to record the freezing time of the mice in the 15 min. D4 was the extinction period; mice were kept in the fear box without foot shock for 5 min to test the freezing time. The extinction coefficient was calculated as previously described: [Extinction coefficient = (1 − (Fear test after 24 (freezing time)/first 3 min block (freezing time))) × 100%] (Gao et al., 2023; Lonsdorf et al., 2019).

2.4. Proteomics analysis

Experiment 1 was used to detect the DEPs in the hippocampus of mice in the Control and SPS groups. This test was completed by Shanghai OE Biotech Co., Ltd (China). In short, 14 days after establishment of the SPS model, the hippocampal tissues of two groups of mice were extracted and the protein concentration was detected. Trypsin-TPCK was added to hydrolyze the hippocampal proteins. The protein samples after enzymatic hydrolysis were labeled. The processed protein samples were analyzed by liquid chromatography (LC)-mass spectrometry (MS)/MS and searched in the database to obtain the original data of the experiment. The DEPs were identified and functional enrichment analysis was performed based on Uniprot, Kyoto Encyclopedia of Genes and Genomes (KEGG), and Gene Ontology (GO) databases.

2.5. Electrophysiology

The experimental method refers to a previous study (Zhu et al., 2018). Following 5% isoflurane anesthesia, the brain was quickly removed and transferred to oxygenated pre-cold cutting fluid (1.25 mM KH_2PO_4, 5 mM $MgSO_4$, 26 mM $NaHCO_3$, 10 mM D-glucose, 3 mM KCl, 124 mM NaCl, and 1.5 mM $CaCl_2$). Hippocampal transversal slices (350 μm thick) were prepared using a vibratome (Leica, Germany), followed by transfer to an interface recording chamber, exposure to a warm and humidified atmosphere with 95% O_2/5% CO_2, and continuous perfusion with oxygen and preheated aCSF (1.5 mM $MgSO_4$, 5 mM KCl, 2.5 mM $CaCl_2$, 110 mM NaCl, 1.24 mM KH_2PO_4, 10 mM D-glucose, and 27.4 mM $NaHCO_3$) at the flow speed of 1.6 mL/min.

After incubation in the recording chamber for 1 h, twisted nichrome wires (single bare wire diameter, 50 μm) were placed in CA1 stratum radiatum, and the field excitatory postsynaptic potentials (fEPSPs) elicited by stimulation of Schaffer collateral pathway were recorded with a single glass pipette filled with 2 M NaCl. The responses were recorded by a differential amplifier (DAM 50, World Precision Instruments, USA) with 10 kHz low-pass and 0.1 Hz high-pass filters. Before each experiment, the input/output (I/O) relationship was checked by changing the stimulus intensity. The data were collected and digitized with Clampex software, and the slope of fEPSP was analyzed. The LTP level was normalized to the average slope of the response recorded during the 10 min baseline, and the responses were recorded at least 40 min after LTP induction.

2.6. Western blot

The hippocampal tissue was placed in an Eppendorf (EP) tube, and 100 μL of RIPA lysate (including 1% phenylmethylsulfonyl fluoride (PMSF)) was added to extract the protein at 4 °C. After loading 5 μL of the protein sample into each well of the gel, protein samples were separated by sodium dodecyl-sulfate polyacrylamide gel electrophoresis (SDS-PAGE) gel electrophoresis (5% concentrated gel: 75 V/15 min, 10% separation gel: 115 V/75 min). The proteins were then transferred to a nitrocellulose membrane at 400 mA for 40 min. Thereafter, the membrane was blocked with 5% skim milk at room temperature. The membrane was incubated with the primary antibodies overnight at 4 °C: β-actin (1:1000, 3700S, Cell Signaling Technology), μ-calpain (1:1000, 10538-1-AP, Proteintech), p-RAC1 (1:500, 310221, ZEN BIO), RAC1 (1:500, 600573, ZEN BIO), p-PAK1 (1:500, 310208, ZEN BIO), PAK1 (1:500, R26170, ZEN BIO), DCC (1:1000, 67203-1-Ig, Proteintech), ARC (1:1000, 66550-1-Ig, Proteintech), and GAPDH (1:1000, 380626, ZEN BIO). The next, the membrane was washed with phosphate-buffered saline with tween (PBST) (3 × 10 min) and incubated with the second antibody (1:10000, peroxidase-conjugated goat anti-rabbit/mouse IgG, ZB-2301/2305, ZSGB-BIO) at room temperature for 2 h. After washing with PBST (3 × 10 min), enhanced chemiluminescence (ECL) chromogenic reagent (Tanon) was applied to detect the proteins. The protein images were analyzed by ImageJ software. After normalization, statistical analysis was conducted.

2.7. Immunofluorescence

The brain tissue was fixed with 4% paraformaldehyde (PFA) and dehydrated. The coronal section was cut into 20 μm slices (bregma: −2.3 mm ± 100 μm, two slices). The brain slices were washed with PBS (3 × 10 min), blocked with 10% goat serum for 1 h, and incubated with the primary antibodies overnight at 4 °C: DCC (1:50) and p-PAK1 (1:50). Thereafter, the brain slices were washed with PBS (3 × 15 min), and the secondary antibody (TRITC-labeled anti-mouse/FITC-labeled anti-rabbit IgG) was incubated at room temperature for 2 h. Finally, the sections were stained for 10 min with 4′,6-diamidino-2-phenylindole (DAPI). After washing with PBS (3 × 15 min), the slices were attached to glass slides, sealed with cover slides, and preserved away from light. The immunofluorescence specimens were observed and photographed by a laser confocal microscope (FV3000, OLYMPUS, Japan). The immunofluorescence images were analyzed using ImageJ software.

2.8. Statistical analysis

The experimental data were analyzed using Graphpad Prism 9.0 software (GraphPad Inc., San Diego, CA, USA). The data were expressed as means ± standard error of the mean (SEM). The independent sample

t-test was used to compare the data of two groups, one-way or two-way ANOVA was used to compare more than two groups of data, and Tukey's test or Dunn's test was used for multiple comparative analysis. When $p < 0.05$, the experiment was considered to be statistically significant.

3. Results

3.1. Hippocampal DCC is elevated in SPS mice

In this study, we first used behavioral tests to confirm the reliability of the SPS model. The EPM results revealed that the open arm time of SPS mice was significantly shorter than that of Control mice ($p < 0.05$, t = 4.922, df = 10), and the closed arm time of SPS mice was longer than that of Control mice ($p < 0.05$, t = 4.884, df = 10) (Fig. 1B and C). In the OFT, the center distance ($p < 0.05$, t = 2.851, df = 10), center time ($p < 0.05$, t = 3.199, df = 10), and center entries ($p < 0.05$, t = 2.379, df = 10) of SPS mice were significantly lower than those of Control mice (Fig. 1D–G). The results of FMT indicated that the freezing time of SPS mice during the extinction session was higher than that of Control mice ($p < 0.05$, t = 3.406, df = 10), which remained at a high level after extinction ($p < 0.05$, t = 3.309, df = 10). In addition, the extinction coefficient showed that the fear memory extinction in SPS mice was lower than that in Control mice ($p < 0.05$, t = 3.239, df = 10) (Fig. 1H–J). These data indicate that the PTSD-like behavior was successfully established in these mice. The follow-up experiments were carried out based on the stability of the SPS model.

After retrieving the original data from the database, the trusted proteins were screened according to the condition of Score Sequest HT > 0 and unique peptide ≥1, and the blank value was removed. Based on trusted proteins, the screening conditions of DEPs were set as follows: fold change (FC) > 1.2 or < 0.83, and *p*-value <0.05. The screening results are shown in Table 1. There were 19 DEPs (10 upregulated and 9 downregulated) between group B (SPS group) and group A (Control group) (Fig. 1 K). A cluster heat map was used to visually display the standardized DEP data (Fig. 1 L).

According to the proteomic analysis of the DEPs, DCC attracted our attention because of its role in regulating synaptic function and emotional disorders (Horn et al., 2013; Popa et al., 2022). Firstly, the changes in the expression of DCC in the hippocampus of SPS mice were verified by western blotting at D0, D1, D7, and D14 in the process of SPS modeling. The results indicated a significant increase in DCC at D14 compared to D0 ($p < 0.05$, $F_{[3, 16]} = 4.410$) (Fig. 1 M). After confirming the dynamic changes in DCC, the expression of the downstream Rac1–Pak1 proteins, which are regulated by DCC, in the hippocampus of mice in Control group and SPS group was detected by western blotting (Li et al., 2002). Dephosphorylation of Rac1 is known to indicate the activation of Rac1 (Kwon et al., 2000). The results revealed that when the hippocampal DCC expression was increased in SPS mice ($p < 0.05$, t = 3.903, df = 10) (Fig. 1 N), the level of downstream p-Rac1 decreased significantly ($p < 0.05$, t = 4.609, df = 10) (Fig. 1 O), and p-Pak1 increased ($p < 0.05$, t = 3.706, df = 10) (Fig. 1 P). The immunofluorescence results showed that the DCC level in the CA1 region ($p < 0.05$, t = 5.769, df = 10) was higher in the SPS group than in the Control group (Fig. 1Q and R). Together, these data suggest that DCC was highly expressed in the hippocampus of SPS mice.

Based on the Uniprot, KEGG, and GO databases, GO/KEGG enrichment analysis were performed on the DEPs. The GO enrichment analysis (including biological process, cellular component, and molecular function) of group A (Control group) and group B (SPS group) is shown in Fig. 1 S. The results of the GO analysis suggested that the DEPs are expressed in synapses and axons, which are related to the regulation of biological processes, such as neuron projection. The bubble diagram of the KEGG enrichment analysis of group A (Control group) and group B (SPS group) is shown in Fig. 1 T. The KEGG analysis suggested that the DEPs are involved in the processes of axon guidance and endocytosis. The results of the proteomics revealed that DCC might be a highly related target for PTSD (Fig. 1 U).

3.2. Increase expression of DCC controls fear memory extinction and hippocampal LTP

A DCC overexpression virus was used to confirm that DCC was the key target of fear memory extinction impairment and anxiety-like behavior in male SPS mice. The results of the EPM showed that, compared with the Scramble group, the open arm time of Scramble + SPS group and OE-DCC group was significantly shorter, and the open arm time ($p < 0.05$, $F_{[3, 24]} = 52.33$) of the OE-DCC + SPS group was also short compared with that of the Scramble + SPS group (Fig. 2B and C). In the OFT, the center distance ($p < 0.05$, $F_{[3, 24]} = 11.65$) and center time ($p < 0.05$, $F_{[3, 24]} = 4.84$) of the Scramble + SPS group and OE-DCC group were lower than those of the Scramble group, and the center distance of the OE-DCC + SPS group was significantly lower than that of the Scramble + SPS group (Fig. 2D–G).

The FMT results showed that fear memory extinction in the Scramble + SPS group and the OE-DCC group was impaired compared with that in the Scramble group. The freezing time in the Scramble + SPS group and the OE-DCC group was higher than that in the Scramble group during the extinction session, and the freezing time in the OE-DCC + SPS group was higher than that in the Scramble + SPS group (group: $p < 0.05$, $F_{[4, 30]} = 45.48$; time: $p < 0.05$, $F_{[2.538, 76.13]} = 18.84$;

Table 1
Differentially expressed proteins in the hippocampus between control and SPS mice.

Accession	Gene Name	Protein Name	groupA1	groupA2	groupB1	groupB2	p-value	FC
P70211	Dcc	Netrin receptor DCC	71.3	70.8	149.4	148.4	5.16E-05	2.095707
Q91X72	Hpx	Hemopexin	78.2	87.2	111.3	108.4	0.029011	1.328295
P02088	Hbb-b1	Hemoglobin subunit beta-1	83.2	90.9	115.1	111.2	0.026269	1.299828
Q8C0Q2	Zhx3	Zinc fingers and homeoboxes protein 3	90.8	84.3	113.7	113.3	0.015382	1.296402
Q8CEE7	Rdh13	Retinol dehydrogenase 13	84.1	89.7	111.3	110.7	0.01338	1.27733
P07758	Serpina1a	Alpha-1-antitrypsin 1-1	87.8	91.8	115.8	112.5	0.011149	1.271158
P01837	Igkc	Immunoglobulin kappa constant	87.2	85.6	111.8	104.4	0.029109	1.251157
Q8R1L4	Kdelr3	ER lumen protein-retaining receptor 3	92	86.1	109.3	111.3	0.020818	1.23863
Q8VCM7	Fgg	Fibrinogen gamma chain	87.6	89.3	107.6	106.9	0.002382	1.212549
Q99J09	Wdr77	Methylosome protein 50	85	92.8	107.1	106.9	0.043452	1.2036
P59823	Il1rapl1	Interleukin-1 receptor accessory protein-like 1	114.5	111	96.2	90.3	0.029574	0.827051
Q8C2E7	Washc5	WASH complex subunit 5	114.4	107.1	88.7	92	0.036459	0.815801
P56183	Rrp1	Ribosomal RNA processing protein 1 homolog A	110.7	119.7	91.6	94.3	0.041809	0.806858
Q6ZWY8	Tmsb10	Thymosin beta-10	117.9	123.3	92.8	89.5	0.011348	0.755804
P02802	Mt1	Metallothionein-1	102.4	100.1	79.8	68	0.045064	0.729877
Q9CY45	Eef1akmt1	EEF1A lysine methyltransferase 1	122.9	114.3	82	84.9	0.016262	0.703626
Q6ZPS6	Ankib1	Ankyrin repeat and IBR domain-containing protein 1	119.1	130.6	84.9	68.5	0.040644	0.614337
P28184	Mt3	Metallothionein-3	133.8	115.6	68.4	65.5	0.024528	0.536889
Q9Z2R6	Unc119	Protein unc-119 homolog A	140.1	145.8	71	81.4	0.0078	0.533054

group × time: $p > 0.05$, $F_{[12, 90]} = 0.451$). After extinction, the freezing time in the Scramble + SPS group and the OE-DCC group was significantly higher than that in the Scramble group ($p < 0.05$, $F_{[3, 24]} = 19.95$). We also calculated the extinction coefficient, which was lower in the Scramble + SPS group and OE-DCC group than that in the Scramble group ($p < 0.05$, $F_{[3, 24]} = 88.83$) (Fig. 2H–J).

The western blotting results revealed that the DCC level in the Scramble + SPS group and the OE-DCC group were significantly higher than that in the Scramble group, and the DCC level in the OE-DCC + SPS group was higher than that in the Scramble + SPS group ($p < 0.05$, $F_{[3, 20]} = 13.19$) (Fig. 2 K). Furthermore, the virus-induced high expression of DCC corresponded to the decrease in p-Rac1 ($p < 0.05$, $F_{[3, 20]} = 27.23$) and the increase in p-Pak1 ($p < 0.05$, $F_{[3, 20]} = 39.79$) (Fig. 2L and M). The injection location of the virus was verified by immunofluorescence (Fig. 2 N). Furthermore, we found that DCC overexpression impaired the LTP in the CA1 region and the 40-min LTP values returned to the baseline level (LTP level at 40 min: *vs.* Scramble, $p < 0.05$, $t = 2.994$, $df = 6$) (Fig. 2O and P). These results suggest that the overexpression of hippocampal DCC could damage fear memory extinction and hippocampal LTP in mice.

3.3. Immunotherapy against DCC improves fear memory extinction in SPS mice

Considering the high level of hippocampal DCC in SPS mice, we verified whether neutralizing antibodies could play a functional inhibitory effect. We first performed immunofluorescence staining without membrane penetration by Triton-100 and confirmed that the antibody could bind to the extracellular domain of hippocampal CA1 pyramidal cells (Fig. 3 B). The results of the behavioral tests showed that the SPS + Anti-DCC(−) group had a significantly shorter open arm time in the EPM compared to the Control + Anti-DCC(−) group. The DCC antibody significantly increased the open arm time ($p < 0.05$, $F_{[3, 20]} = 12.25$) in SPS mice (Fig. 3C and D). In the OFT, the central distance ($p < 0.05$, $F_{[3, 20]} = 5.888$) and center entries ($p < 0.05$, $F_{[3, 20]} = 15.98$) in SPS + Anti-DCC(−) group were lower than those in Control + Anti-DCC(−) group. Following the inhibition of DCC, the center distance and center time of SPS mice were enhanced (Fig. 3E–**H**). The FMT also showed that inhibition of DCC could also improve fear memory extinction in SPS mice (group: $p < 0.05$, $F_{[4, 25]} = 41.87$; time: $p < 0.05$, $F_{[2.30, 57.52]} = 27.56$; group × time: $p > 0.05$, $F_{[12, 75]} = 0.41$). After extinction, the freezing time in the SPS + Anti-DCC(−) group was significantly higher than that in the SPS + Anti-DCC(+) ($p < 0.05$, $F_{[3, 20]} = 43.56$). The results of the extinction coefficient further supported that inhibiting DCC could improve fear memory extinction in SPS mice ($p < 0.05$, $F_{[3, 20]} = 43.89$) (Fig. 3I–**K**). Additionally, the DCC antibody did not affect the anxiety-like behavior and fear memory extinction in Control mice. These data suggest that the immunotherapy against DCC improves PTSD-like behavior in SPS mice.

3.4. SPS-induced increase in DCC is likely caused by the weakening of μ-calpain cleavage

We used a μ-calpain KD virus and the calpain inhibitor calpeptin to further investigate the causation of DCC elevation in male SPS mice. The Western blot results revealed that μ-calpain expression was decreased in the μ-calpain KD group and μ-calpain KD + SPS group compared to the in Scramble group (**S 1 B-C**), DCC expression was increased in the μ-calpain KD group and μ-calpain KD + SPS group compared to the Scramble group, and that DCC expression was increased in the μ-calpain KD + SPS group compared to the μ-calpain KD group (**S 1 D**).

Chronic administration of calpeptin caused anxiety-like behavior in Control mice, as shown in the OFT but not in the EPM (Fig. 4B–G). The results of the FMT revealed that in the extinction session, the freezing time ion the SPS group was higher than that in the Control group, and calpeptin could also significantly increase the freezing time in the Control group ($p < 0.05$, $F_{[3, 24]} = 6.699$). Furthermore, the extinction coefficient in Control mice was reduced after calpeptin administration ($p < 0.05$, $F_{[3, 24]} = 7.459$) (Fig. 4H–J). The Western blot results of experiment 5 revealed that the levels of μ-calpain in the SPS group and Control + Calpeptin group were lower than that in the Control group ($p < 0.05$, $F_{[3, 20]} = 95.51$) (Fig. 4K and L); however, the level of DCC in the SPS group and SPS + Calpeptin group was higher than that in the Control group, and the level of DCC in the SPS + Calpeptin group was higher than that in the SPS group ($p < 0.05$, $F_{[3, 20]} = 36.28$) (Fig. 4 M). These data indicate that the level of DCC increased after calpain inhibition. Therefore, biochemical and behavioral test together indicate that chronic inhibition of μ-calpain can contribute to the increased expression of DCC and PTSD-like behaviors in mice.

3.5. NSC23766 rescues fear memory extinction and regulates synaptic function in SPS mice

The RAC1–PAK1 signaling pathway is a well verified to occur downstream of DCC (Li et al., 2002). To confirm that DCC is the key mechanism for fear memory extinction of SPS mice, we further investigated whether antagonizing the Rac1-Pak1 signaling pathway with NSC23766 could improve the behavioral changes. The results of the EPM revealed that NSC23766 significantly increased the open arm time ($p < 0.05$, $F_{[2, 15]} = 24.01$) and decreased the closed arm time ($p < 0.05$, $F_{[2, 15]} = 25.86$) in SPS mice (Fig. 5B and C). In the OFT, NSC23766 significantly increased the center distance ($p < 0.05$, $F_{[2, 15]} = 6.229$), center time ($p < 0.05$, $F_{[2, 15]} = 7.656$), and center entries ($p < 0.05$, $F_{[2, 15]} = 4.976$) in the SPS group (Fig. 5D–G). In the FMT, NSC23766 improved fear memory extinction of SPS mice (after extinction: vs SPS, $p < 0.05$, $F_{[2, 15]} = 9.993$; extinction coefficient: vs SPS, $p < 0.05$, $F_{[2, 15]} = 40.80$) (Fig. 5H–J). These data suggest that the inhibition of Rac1 with NSC23766 rescues the impairment of fear memory extinction in SPS mice.

The results showed that the level of p-Rac1 in the SPS group was lower than that in Control group, and the level of p-Pak1 was higher than that in Control group. NSC23766 increased the level of p-Rac1 ($p < 0.05$, $F_{[2, 15]} = 16.31$) and decreased the expression of p-Pak1 ($p < 0.05$, $F_{[2, 15]} = 9.456$) in the hippocampus of SPS mice (Fig. 5K and L). The immunofluorescence results showed that the number of p-Pak1 puncta and the total area of p-Pak1 puncta in the SPS group were higher than those in the Control group; however, NSC23766 reduced the number of p-Pak1 puncta ($p < 0.05$, $F_{[2, 15]} = 13.75$) and the total area of p-Pak1 puncta ($p < 0.05$, $F_{[2, 15]} = 9.192$) in SPS mice (Fig. 5M–O). The result was consistent with the expression of p-Pak1 detected by western blotting. Electrophysiological results showed that hippocampal LTP was impaired in the SPS group, which was prohibited by administration of NSC23766 ($p < 0.05$, $F_{[2, 9]} = 8.091$) (Fig. 5P and Q). The expression of Arc protein also indicated that the damaged synaptic function of SPS mice was rescued by the administration of NSC23766 ($p < 0.05$, $F_{[2, 15]} = 23.40$) (Fig. 5 R).

4. Discussion

In this study, we firstly assessed whether hippocampal DCC expression was elevated in mice receiving SPS based on proteomics. Later, we confirmed that the increased level of hippocampal DCC contributed to the impairment of fear memory extinction. This study also revealed that the decrease in cleavage effect caused by μ-calpain inhibition might be one reason for the elevation in the DCC level. Additionally, antagonizing the Rac1-Pak1 signaling pathway downstream of DCC could remedy the impairment of fear memory extinction and hippocampal LTP in male mice receiving SPS. Our results provide novel ideas for the recognition of PTSD, in addition to potential therapeutic targets.

4.1. DEPs in the hippocampus provide therapeutic targets for PTSD

An excessively strong response to stressors may be associated with abnormal activity in the CA1 region (Jimenez et al., 2020). The activity of neurons in the hippocampal CA1 region is believed to be involved in the encoding and retrieval of fear memory. Chronic stress, whether in familiar or novel environments, can disrupt the acuity and specificity of encoding in the CA1 region, altering hippocampal oscillations (Tomar and McHugh, 2022). Animal models of PTSD exhibit a significant reduction in the volume of the CA1 region and the number of pyramidal cells, while the nuclear/cytoplasmic ratio of pyramidal cells increases (Feng et al., 2020; Smith et al., 2019). Similarly, magnetic resonance imaging (MRI) of the brains of PTSD patients shows a reduction in the volume of the hippocampal CA1 region; this morphological change is associated with an exacerbation of anxiety-like behaviors (Chen et al., 2018). Previously, we identified structural and biochemical changes in the hippocampus of the mice receiving SPS, including pyramidal neuronal apoptosis, astrocyte atrophy, and dysregulation of synaptic proteins (Wang et al., 2022). Therefore, this experiment continued to focus on investigating the mechanism in the CA1 region. Since protein function depends on post-translational modifications and varies with protein localization, proteomics is of great significance to fully understand the working principle of biological systems (Altelaar et al., 2013). In this study, proteomic techniques were used to screen hippocampal DEPs between SPS mice and Control mice. In total, 19 hippocampal DEPs were identified in the mice receiving SPS, including 10 upregulated and nine downregulated proteins. We speculate that those 19 DEPs are key proteins determining hippocampal function in PTSD. Among the DEPs was protein uncoordinated 119 (UNC119), which is required for G protein transport in sensory neurons; *UNC119* deletion could lead to incorrect localization of G proteins (Zhang et al., 2011). Dendritic structural defects are common in neuropsychiatric disorders; Il1rapl1 is located at excitatory synapses and is involved in X-linked cognitive impairment by regulating the function of dendrites (Montani et al., 2017). Furthermore, we identified metallothionein-1 (MT-1), which has neuroprotective effects (Miyazaki et al., 2013). Undoubtedly, a full investigation of the DEPs will facilitate the understanding of the cognitive function in patients with PTSD. Through GO and KEGG enrichment analysis, we observed that the DEPs were enriched in the synapse and axon of neurons, affecting the process of protein transport, and regulating the function of molecular signal receptors. In the subsequent experiments, we focused on DCC and synaptic function during PTSD development.

4.2. DCC is a key potential target for controlling hippocampal LTP and fear memory extinction in SPS mice

A study of postmortem brain tissue from patients with major depression and depressed mice revealed that DCC overexpression was a common feature of depression, and that upregulation of DCC led to susceptibility in mice (Torres-Berrío et al., 2017). GWAS analysis of risk genes for major depressive disorder based on large sample data also revealed significant differences in *DCC* gene expression for depression in different populations. Further analysis of the biological processes showed that DCC also regulates synaptic plasticity, axonal guidance, circadian rhythm, and LTP (Li et al., 2020). These data together suggest that DCC may be one potential factor for the symptoms and impairment of synaptic function in PTSD.

PTSD is a psychiatric disorder that occurs with a delay following a stressful event (Amos et al., 2014). In this study, we found that the expression levels of DCC were low in the hippocampus of mice when they were not exposed to SPS or in the short term after stimulation (D0, D1, and D7). However, 14 days after the stress stimulation, the mice displayed obvious impaired fear memory extinction, which was accompanied with an abrupt increase in DCC. Therefore, DCC may be an important inducer for the delayed onset of PTSD. To validate this hypothesis, this study further investigated the critical roles of DCC in the hippocampal function. We localized injection of the virus into the hippocampal CA1 region to overexpress DCC in the $CaMKII^{+}$ cells, thus confirming that the increased expression of DCC is an inducer of impaired fear memory extinction and anxiety-like behavior. Indeed, overexpression of DCC not only induced a similar behavior to SPS itself, it also aggravated the action of SPS. Furthermore, we found that overexpression of DCC activated the Rac1-Pak1 signaling pathway and impaired hippocampal LTP. Based on previous publications (Cramer et al., 2023; Horn et al., 2013), DCC was found to be expressed in both excitatory and inhibitory neurons. Selective knockdown of DCC in $CaMKII^{+}$ neurons in the hippocampus reduced Src activation and thus inhibited N-methyl-D-aspartate receptor (Nmdar) function, resulting in impaired LTP in mice (Horn et al., 2013). In the present study, we first reported that overexpression of DCC in hippocampal $CaMKII^{+}$ neurons could stimulate PTSD-like phenotypes, and even aggravate the detriment effect of SPS. Importantly, overexpression of DCC also impaired hippocampal LTP. Although DCC is important for LTP induction (Cramer et al., 2023), a high level of DCC under pathological conditions could also be detriment for hippocampal LTP. Electrophysiological data from experiment 2 indicated that overexpression of DCC disrupts LTP in normal mice; the values returned to baseline levels by 40 min. Given that DCC overexpression might obscure the effects of SPS, experiment 2 only assessed the Scramble group and OE-DCC group. However, results from experiment 6 demonstrated that SPS modeling also impairs LTP, consistent with the LTP result of experiment 2. This corroborated our conclusions.

Later, neutralizing antibody experiments used the mouse-derived DCC monoclonal antibody to assess whether inhibition of DCC could improve the behavioral changes in SPS mice. As expected, the impaired fear memory extinction of SPS mice was improved following the inhibition of DCC. The results of this study suggest, for the first time, that DCC is a critical target responsible for impaired fear memory extinction in SPS mice.

4.3. Elevation of DCC is likely caused by μ-calpain inhibition elicited by SPS exposure

Although the inflammatory response and dysfunction of the hypothalamic–pituitary–adrenal axis have been proposed as the main mechanisms for the pathogenesis of PTSD, structural and function modulation of synapses is the core mechanism for psychiatric disorders (Sanacora et al., 2022). In a previous study, we found that the expression of μ-calpain decreased 1 day after SPS modeling, which continued until the appearance of abnormal behavioral function (Wang et al., 2022). The function of calpain in synaptic plasticity has been well investigated, especially in LTP and long-term depression (LTD) (Zhu et al., 2017). Therefore, the reduction of μ-calpain may also have led to LTP impairment. Additionally, it has been demonstrated that μ-calpain can cleave DCC, resulting in the degradation of DCC (Duquette and Lamarche-Vane, 2020). The prolonged inhibition of μ-calpain may be one reason for the increase in the DCC level after SPS. This point of view was further supported by the viral knockdown of μ-calpain and chronic administration of calpeptin. Viral knockdown of μ-calpain resulted in the elevation of DCC. Meanwhile, chronic administration of calpeptin, an inhibitor of both μ-calpain and m-calpain, also led to an increase in the DCC level. Therefore, both genetic and pharmacological methods implicated that the abrupt elevation of DCC might be caused by calpain inhibition. μ-calpain is required for neurodevelopment in mammals, and its deletion leads to cerebellar ataxia (Wang et al., 2016) and mental disorders (Song et al., 2019). In our study, we found that chronic administration of calpeptin (2 mg/kg) could impair fear extinction and cause anxiety-like behavior. These data were consistent with previous publications, which emphasizes the importance of calpain in fear memory (Nagayoshi et al., 2017). Additionally, although calpain inhibitors are potential medications for neurological disorders, long-term

application might also cause PTSD-related symptoms.

The level of biological proteins is regulated by both synthesis and degradation pathways (Raffeiner et al., 2023). In addition to μ-calpain-mediated degradation of DCC, elevated DCC expression may also be associated with increased protein synthesis. It was shown that miR-218, a post-transcriptional repressor of DCC, was co-expressed with DCC in pre-frontal cortex (PFC) pyramidal neurons, and decreased miR-218 levels could upregulate the expression of DCC in the PFC (Torres-Berrío et al., 2017). The cause of elevated DCC in SPS mice remains an unsolved mystery. In subsequent studies, we will continue to reveal the reasons for the rise of DCC from an epigenetic perspective and provide more evidence for DCC as a therapeutic target for PTSD.

4.4. DCC regulates hippocampal synaptic function through the Rac1–Pak1 signaling pathway

Synaptic plasticity, especially LTP, has been recognized as an important component of learning and memory (Neves et al., 2008). It has been suggested that the maintenance of contextual fear memory is regulated by hippocampal brain regions and that the strength of the therapeutic effect of PTSD exposure therapy is critically dependent on the role of the hippocampus (Chaaya et al., 2018). Our previous study found that hippocampal synaptic dysfunction was directly related to the occurrence of PTSD. The Bdnf–TrkB signaling pathway and synapse related proteins (Psd95, GluA1, and p-Mtor) were reduced in the hippocampus of SPS mice compared to normal mice, in addition to a reduction in the GluN2A/GluN2B ratio (Wang et al., 2022). The changes in these synaptic proteins led to impairment of hippocampal LTP in the SPS model (Diering and Huganir, 2018). Similarly, the occurrence of PTSD has been shown to be associated with hippocampal synaptic function in several other studies by our team (Ji et al., 2023).

It has been reported that DCC can independently activate RAC1 to reconstruct the actin cytoskeleton (Shekarabi and Kennedy, 2002). Furthermore, RAC1 plays a critical role in regulating neuronal structure, synaptic plasticity, and memory (Hayashi-Takagi et al., 2015). During the maintenance period of LTP, RAC1 can be activated by an adeno-associated virus carrying the transgene, resulting in an accelerated decline of hippocampal LTP (Liu et al., 2016). Another study reported that excessive activation of Rac1 in hippocampal neurons induced memory deficits in APP/PS1 mice; however, inhibition of Rac1 activity enhanced LTP and improved memory deficits (Wu et al., 2019). This suggests that RAC1 could affect LTP to improve memory function. Our study found that the Rac1-Pak1 signaling pathway was activated following the increase in hippocampal DCC in SPS mice, while the inhibition of Rac1-Pak1 by NSC23766 not only improved the impaired fear memory extinction in SPS mice, but also rescued the impaired LTP in the hippocampus. Accordingly, our study proposes a hypothesis that hippocampal DCC impairs synaptic function through activation of the RAC1-PAK1 signaling pathway and is involved in fear memory abnormalities in PTSD (Fig. 6).

4.5. Research shortcomings and outlook

The neutralizing antibody method used in the experiment is effective for the inhibition of DCC in mice; however, it is still difficult and challenging to apply in the clinical treatment of PTSD. Unfortunately, we did not identify any DCC inhibitors and were unable to evaluate whether DCC inhibitors could be used as potential therapeutic agents for PTSD. Therefore, DCC inhibitors could be prodrugs for the treatment of PTSD, which is of significance for the development of new drugs. In addition, synaptic proteins are important bearers of synaptic function, and LTP is the physiological basis of learning and memory (Nabavi et al., 2014). Although this study has revealed that DCC regulates synaptic defects and impairs LTP through activation of RAC1-PAK1, the regulatory effect of DCC on LTP in other brain regions related to fear memory, such as the amygdala and PFC, remain unclear, requiring future investigations. Finally, whether DCC plays the same role in female mice needs to be further verified, as female PTSD accounts most of the population.

5. Conclusions

In summary, our study reports that DCC regulated by calpain is critical in the control of hippocampal LTP and PTSD-like behavior, which is indicated to act through the RAC1-PAK1 signaling pathway. This study provides a potential membrane target for the future therapeutics for PTSD.

Availability of data and materials

All the data supporting this study's findings are available from the corresponding authors upon reasonable request.

CRediT authorship contribution statement

Shaojie Yang: Writing – original draft, Investigation, Data curation. **Jiamin Hu:** Writing – original draft, Investigation, Data curation. **Yuzhuang Chen:** Methodology. **Zhengrong Zhang:** Methodology. **Jingji Wang:** Methodology. **Guoqi Zhu:** Writing – review & editing, Project administration.

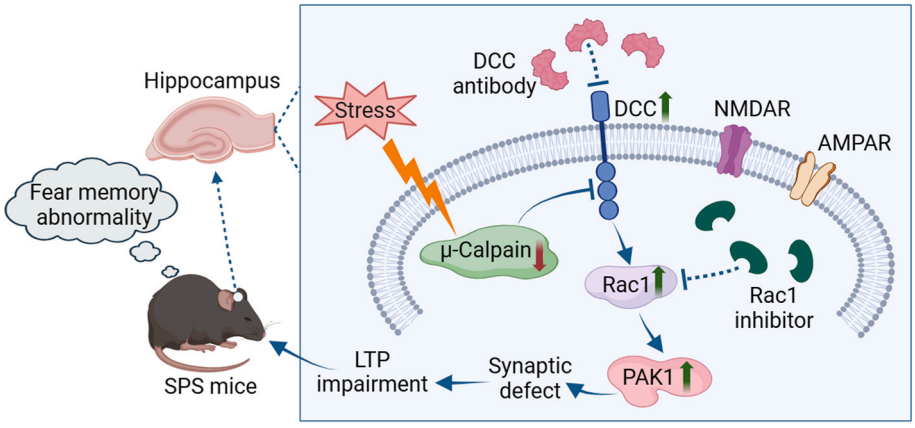

Fig. 6. A schematic illustrates the mechanism. Stress could inhibit the expression of μ-Calpain in hippocampus, thus reduce the cleavage effect of μ-Calpain on DCC, activate downstream Rac1-PAK1 signaling pathway, damage LTP, and induce fear memory abnormality in SPS mice, but DCC antibody and Rac1 inhibitor could improve the fear memory abnormality in SPS mice (Created with BioRender.com).

Declaration of competing interest

The authors declare that they have no known competing financial interests or personal relationships that could have appeared to influence the work reported in this paper.

Data availability

Data will be made available on request.

Acknowledgements

This research was supported by Research Funds of Center for Xin'an Medicine and Modernization of Traditional Chinese Medicine of IHM (2023CXMMTCM013, 2023CXMMTCM021), Anhui Natural Science Foundation (2208085MH282), Excellent Funding for Academic and Scientific Research Activities for Academic and Technological Leaders in Anhui Province (2022D317), Key Project of Anhui Natural Science Research (2022AH050462, 2023AH050758), Talent Research Funding Program (0500-52-1), and Natural Science Research Project of Anhui University of Chinese Medicine (2021zryb04). This research also received the help and support of Professor Ming Chen of Fudan University.

Appendix A. Supplementary data

Supplementary data to this article can be found online at https://doi.org/10.1016/j.ynstr.2024.100666.

References

Altelaar, A.F., Munoz, J., Heck, A.J., 2013. Next-generation proteomics: towards an integrative view of proteome dynamics. Nat. Rev. Genet. 14 (1), 35–48. https://doi.org/10.1038/nrg3356.

Amos, T., Stein, D.J., Ipser, J.C., 2014. Pharmacological interventions for preventing post-traumatic stress disorder (PTSD). Cochrane Database Syst. Rev. (7), Cd006239 https://doi.org/10.1002/14651858.CD006239.pub2.

Chaaya, N., Battle, A.R., Johnson, L.R., 2018. An update on contextual fear memory mechanisms: transition between Amygdala and Hippocampus. Neurosci. Biobehav. Rev. 92, 43–54. https://doi.org/10.1016/j.neubiorev.2018.05.013.

Charlson, F., van Ommeren, M., Flaxman, A., Cornett, J., Whiteford, H., Saxena, S., 2019. New WHO prevalence estimates of mental disorders in conflict settings: a systematic review and meta-analysis. Lancet (London, England) 394, 240–248. https://doi.org/10.1016/s0140-6736(19)30934-1, 10194.

Chen, L.W., Sun, D., Davis, S.L., Haswell, C.C., Dennis, E.L., Swanson, C.A., Whelan, C.D., Gutman, B., Jahanshad, N., Iglesias, J.E., Thompson, P., Wagner, H.R., Saemann, P., LaBar, K.S., Morey, R.A., 2018. Smaller hippocampal CA1 subfield volume in posttraumatic stress disorder. Depress. Anxiety 35 (11), 1018–1029. https://doi.org/10.1002/da.22833.

Chen, Y., Wang, X., Xiao, B., Luo, Z., Long, H., 2023. Mechanisms and functions of activity-regulated cytoskeleton-associated protein in synaptic plasticity. Mol. Neurobiol. 60 (10), 5738–5754. https://doi.org/10.1007/s12035-023-03442-4.

Cramer, T.M.L., Pinan-Lucarre, B., Cavaccini, A., Damilou, A., Tsai, Y.C., Bhat, M.A., Panzanelli, P., Rama, N., Mehlen, P., Benke, D., Karayannis, T., Bessereau, J.L., Tyagarajan, S.K., 2023. Adamtsl3 mediates DCC signaling to selectively promote GABAergic synapse function. Cell Rep. 42 (8), 112947 https://doi.org/10.1016/j.celrep.2023.112947.

Diering, G.H., Huganir, R.L., 2018. The AMPA receptor code of synaptic plasticity. Neuron 100 (2), 314–329. https://doi.org/10.1016/j.neuron.2018.10.018.

Duquette, P.M., Lamarche-Vane, N., 2020. The calcium-activated protease calpain regulates netrin-1 receptor deleted in colorectal cancer-induced axon outgrowth in cortical neurons. J. Neurochem. 152 (3), 315–332. https://doi.org/10.1111/jnc.14837.

Feng, D.Y., Guo, B.L., Liu, G.H., Xu, K., Yang, J., Tao, K., Huang, J., Wang, L.Y., Wang, W., Wu, S.X., 2020. Nerve growth factor against PTSD symptoms: preventing the impaired hippocampal cytoarchitectures. Progress in neurobiology 184, 101721. https://doi.org/10.1016/j.pneurobio.2019.101721.

Frankland, P.W., Josselyn, S.A., 2016. Hippocampal neurogenesis and memory clearance. Neuropsychopharmacology 41 (1), 382–383. https://doi.org/10.1038/npp.2015.243.

Gao, F., Wang, J., Yang, S., Ji, M., Zhu, G., 2023. Fear extinction induced by activation of PKA ameliorates anxiety-like behavior in PTSD mice. Neuropharmacology 222, 109306. https://doi.org/10.1016/j.neuropharm.2022.109306.

Hallock, H.L., Quillian, H.M.t., Maynard, K.R., Mai, Y., Chen, H.Y., Hamersky, G.R., Shin, J.H., Maher, B.J., Jaffe, A.E., Martinowich, K., 2020. Molecularly defined hippocampal inputs regulate population dynamics in the prelimbic cortex to suppress context fear memory retrieval. Biol. Psychiatr. 88 (7), 554–565. https://doi.org/10.1016/j.biopsych.2020.04.014.

Hayashi-Takagi, A., Yagishita, S., Nakamura, M., Shirai, F., Wu, Y.I., Loshbaugh, A.L., Kuhlman, B., Hahn, K.M., Kasai, H., 2015. Labelling and optical erasure of synaptic memory traces in the motor cortex. Nature 525 (7569), 333–338. https://doi.org/10.1038/nature15257.

Horn, K.E., Glasgow, S.D., Gobert, D., Bull, S.J., Luk, T., Girgis, J., Tremblay, M.E., McEachern, D., Bouchard, J.F., Haber, M., Hamel, E., Krimpenfort, P., Murai, K.K., Berns, A., Doucet, G., Chapman, C.A., Ruthazer, E.S., Kennedy, T.E., 2013. DCC expression by neurons regulates synaptic plasticity in the adult brain. Cell Rep. 3 (1), 173–185. https://doi.org/10.1016/j.celrep.2012.12.005.

Ji, M., Zhang, Z., Gao, F., Yang, S., Wang, J., Wang, X., Zhu, G., 2023. Curculigoside rescues hippocampal synaptic deficits elicited by PTSD through activating cAMP-PKA signaling. Phytother Res. 37 (2), 759–773. https://doi.org/10.1002/ptr.7658.

Jimenez, J.C., Berry, J.E., Lim, S.C., Ong, S.K., Kheirbek, M.A., Hen, R., 2020. Contextual fear memory retrieval by correlated ensembles of ventral CA1 neurons. Nat. Commun. 11 (1), 3492. https://doi.org/10.1038/s41467-020-17270-w.

Kwon, T., Kwon, D.Y., Chun, J., Kim, J.H., Kang, S.S., 2000. Akt protein kinase inhibits Rac1-GTP binding through phosphorylation at serine 71 of Rac1. J. Biol. Chem. 275 (1), 423–428. https://doi.org/10.1074/jbc.275.1.423.

Li, H.J., Qu, N., Hui, L., Cai, X., Zhang, C.Y., Zhong, B.L., Zhang, S.F., Chen, J., Xia, B., Wang, L., Jia, Q.F., Li, W., Chang, H., Xiao, X., Li, M., Li, Y., 2020. Further confirmation of netrin 1 receptor (DCC) as a depression risk gene via integrations of multi-omics data. Transl. Psychiatry 10 (1), 98. https://doi.org/10.1038/s41398-020-0777-y.

Li, X., Saint-Cyr-Proulx, E., Aktories, K., Lamarche-Vane, N., 2002. Rac1 and Cdc42 but not RhoA or Rho kinase activities are required for neurite outgrowth induced by the Netrin-1 receptor DCC (deleted in colorectal cancer) in N1E-115 neuroblastoma cells. J. Biol. Chem. 277 (17), 15207–15214. https://doi.org/10.1074/jbc.M109913200.

Liu, Y., Du, S., Lv, L., Lei, B., Shi, W., Tang, Y., Wang, L., Zhong, Y., 2016. Hippocampal activation of Rac1 regulates the forgetting of object recognition memory. Curr. Biol. 26 (17), 2351–2357. https://doi.org/10.1016/j.cub.2016.06.056.

Lonsdorf, T.B., Merz, C.J., Fullana, M.A., 2019. Fear extinction retention: is it what we think it is? Biol. Psychiatr. 85 (12), 1074–1082. https://doi.org/10.1016/j.biopsych.2019.02.011.

Lu, X., Liu, H., Cai, Z., Hu, Z., Ye, M., Gu, Y., Wang, Y., Wang, D., Lu, Q., Shen, Z., Shen, X., Huang, C., 2022. ERK1/2-dependent BDNF synthesis and signaling is required for the antidepressant effect of microglia stimulation. Brain Behav. Immun. 106, 147–160. https://doi.org/10.1016/j.bbi.2022.08.005.

Mehlen, P., Mazelin, L., 2003. The dependence receptors DCC and UNC5H as a link between neuronal guidance and survival. Biol. Cell. 95 (7), 425–436. https://doi.org/10.1016/s0248-4900(03)00072-8.

Miyazaki, I., Asanuma, M., Murakami, S., Takeshima, M., Torigoe, N., Kitamura, Y., Miyoshi, K., 2013. Targeting 5-HT(1A) receptors in astrocytes to protect dopaminergic neurons in Parkinsonian models. Neurobiol. Dis. 59, 244–256. https://doi.org/10.1016/j.nbd.2013.08.003.

Montani, C., Ramos-Brossier, M., Ponzoni, L., Gritti, L., Cwetsch, A.W., Braida, D., Saillour, Y., Terragni, B., Mantegazza, M., Sala, M., Verpelli, C., Billuart, P., Sala, C., 2017. The X-linked intellectual disability protein IL1RAPL1 regulates dendrite complexity. J. Neurosci. : the official journal of the Society for Neuroscience 37 (28), 6606–6627. https://doi.org/10.1523/jneurosci.3775-16.2017.

Morcom, L., Gobius, I., Marsh, A.P., Suárez, R., Lim, J.W., Bridges, C., Ye, Y., Fenlon, L. R., Zagar, Y., Douglass, A.M., Donahoo, A.S., Fothergill, T., Shaikh, S., Kozulin, P., Edwards, T.J., Cooper, H.M., Sherr, E.H., Chédotal, A., Leventer, R.J., Lockhart, P.J., Richards, L.J., 2021. DCC regulates astroglial development essential for telencephalic morphogenesis and corpus callosum formation. Elife 10. https://doi.org/10.7554/eLife.61769.

Nabavi, S., Fox, R., Proulx, C.D., Lin, J.Y., Tsien, R.Y., Malinow, R., 2014. Engineering a memory with LTD and LTP. Nature 511 (7509), 348–352. https://doi.org/10.1038/nature13294.

Nagayoshi, T., Isoda, K., Mamiya, N., Kida, S., 2017. Hippocampal calpain is required for the consolidation and reconsolidation but not extinction of contextual fear memory. Mol. Brain 10 (1), 61. https://doi.org/10.1186/s13041-017-0341-8.

Neves, G., Cooke, S.F., Bliss, T.V., 2008. Synaptic plasticity, memory and the hippocampus: a neural network approach to causality. Nat. Rev. Neurosci. 9 (1), 65–75. https://doi.org/10.1038/nrn2303.

Oh, J.P., Han, J.H., 2020. A critical role of hippocampus for formation of remote cued fear memory. Mol. Brain 13 (1), 112. https://doi.org/10.1186/s13041-020-00652-y.

Osborne, P.B., Halliday, G.M., Cooper, H.M., Keast, J.R., 2005. Localization of immunoreactivity for deleted in colorectal cancer (DCC), the receptor for the guidance factor netrin-1, in ventral tier dopamine projection pathways in adult rodents. Neuroscience 131 (3), 671–681. https://doi.org/10.1016/j.neuroscience.2004.11.043.

Popa, N., Bachar, D., Roberts, A.C., Santangelo, A.M., Gascon, E., 2022. Region-specific microRNA alterations in marmosets carrying SLC6A4 polymorphisms are associated with anxiety-like behavior. EBioMedicine 82, 104159. https://doi.org/10.1016/j.ebiom.2022.104159.

Raffeiner, M., Zhu, S., González-Fuente, M., Üstün, S., 2023. Interplay between autophagy and proteasome during protein turnover. Trends Plant Sci. 28 (6), 698–714. https://doi.org/10.1016/j.tplants.2023.01.013.

Richter-Levin, G., Stork, O., Schmidt, M.V., 2018. Animal models of PTSD: a challenge to be met. Mol. Psychiatr. 24 (8), 1135–1156. https://doi.org/10.1038/s41380-018-0272-5.

Robinson, R.A., Griffiths, S.C., van de Haar, L.L., Malinauskas, T., van Battum, E.Y., Zelina, P., Schwab, R.A., Karia, D., Malinauskaite, L., Brignani, S., van den

Munkhof, M.H., Düdükcü, Ö., De Ruiter, A.A., Van den Heuvel, D.M.A., Bishop, B., Elegheert, J., Aricescu, A.R., Pasterkamp, R.J., Siebold, C., 2021. Simultaneous binding of Guidance Cues NET1 and RGM blocks extracellular NEO1 signaling. Cell 184 (8), 2103–2120.e2131. https://doi.org/10.1016/j.cell.2021.02.045.

Sanacora, G., Yan, Z., Popoli, M., 2022. The stressed synapse 2.0: pathophysiological mechanisms in stress-related neuropsychiatric disorders. Nat. Rev. Neurosci. 23 (2), 86–103. https://doi.org/10.1038/s41583-021-00540-x.

Sha, Z., Yang, Y., Liu, R., Bao, H., Song, S., Dong, J., Guo, M., Zhao, Y., Liu, H., Ding, G., 2022. Hepatic ischemia-reperfusion injury in mice was alleviated by Rac1 inhibition - more than just ROS-inhibition. Journal of clinical and translational hepatology 10 (1), 42–52. https://doi.org/10.14218/jcth.2021.00057.

Shekarabi, M., Kennedy, T.E., 2002. The netrin-1 receptor DCC promotes filopodia formation and cell spreading by activating Cdc42 and Rac1. Molecular and cellular neurosciences 19 (1), 1–17. https://doi.org/10.1006/mcne.2001.1075.

Smith, K.L., Kassem, M.S., Clarke, D.J., Kuligowski, M.P., Bedoya-Pérez, M.A., Todd, S. M., Lagopoulos, J., Bennett, M.R., Arnold, J.C., 2019. Microglial cell hyper-ramification and neuronal dendritic spine loss in the hippocampus and medial prefrontal cortex in a mouse model of PTSD. Brain Behav. Immun. 80, 889–899. https://doi.org/10.1016/j.bbi.2019.05.042.

Song, Z., Shen, F., Zhang, Z., Wu, S., Zhu, G., 2020. Calpain inhibition ameliorates depression-like behaviors by reducing inflammation and promoting synaptic protein expression in the hippocampus. Neuropharmacology 174, 108175. https://doi.org/10.1016/j.neuropharm.2020.108175.

Song, Z.J., Yang, S.J., Han, L., Wang, B., Zhu, G., 2019. Postnatal calpeptin treatment causes hippocampal neurodevelopmental defects in neonatal rats. Neural regeneration research 14 (5), 834–840. https://doi.org/10.4103/1673-5374.249231.

Stein, M.B., Jain, S., Simon, N.M., West, J.C., Marvar, P.J., Bui, E., He, F., Benedek, D.M., Cassano, P., Griffith, J.L., Howlett, J., Malgaroli, M., Melaragno, A., Seligowski, A.V., Shu, I.W., Song, S., Szuhany, K., Taylor, C.T., Ressler, K.J., 2021. Randomized, placebo-controlled trial of the angiotensin receptor antagonist losartan for posttraumatic stress disorder. Biol. Psychiatr. 90 (7), 473–481. https://doi.org/10.1016/j.biopsych.2021.05.012.

Tomar, A., McHugh, T.J., 2022. The impact of stress on the hippocampal spatial code. Trends Neurosci. 45 (2), 120–132. https://doi.org/10.1016/j.tins.2021.11.005.

Torres-Berrío, A., Lopez, J.P., Bagot, R.C., Nouel, D., Dal Bo, G., Cuesta, S., Zhu, L., Manitt, C., Eng, C., Cooper, H.M., Storch, K.F., Turecki, G., Nestler, E.J., Flores, C., 2017. DCC confers susceptibility to depression-like behaviors in humans and mice and is regulated by miR-218. Biol. Psychiatr. 81 (4), 306–315. https://doi.org/10.1016/j.biopsych.2016.08.017.

Wang, J., Gao, F., Cui, S., Yang, S., Gao, F., Wang, X., Zhu, G., 2022. Utility of 7,8-dihydroxyflavone in preventing astrocytic and synaptic deficits in the hippocampus elicited by PTSD. Pharmacol. Res. 176, 106079 https://doi.org/10.1016/j.phrs.2022.106079.

Wang, Y., Hersheson, J., Lopez, D., Hammer, M., Liu, Y., Lee, K.H., Pinto, V., Seinfeld, J., Wiethoff, S., Sun, J., Amouri, R., Hentati, F., Baudry, N., Tran, J., Singleton, A.B., Coutelier, M., Brice, A., Stevanin, G., Durr, A., Bi, X., Houlden, H., Baudry, M., 2016. Defects in the CAPN1 gene result in alterations in cerebellar development and cerebellar ataxia in mice and humans. Cell Rep. 16 (1), 79–91. https://doi.org/10.1016/j.celrep.2016.05.044.

Ward, J., Strawbridge, R.J., Bailey, M.E.S., Graham, N., Ferguson, A., Lyall, D.M., Cullen, B., Pidgeon, L.M., Cavanagh, J., Mackay, D.F., Pell, J.P., O'Donovan, M., Escott-Price, V., Smith, D.J., 2017. Genome-wide analysis in UK Biobank identifies four loci associated with mood instability and genetic correlation with major depressive disorder, anxiety disorder and schizophrenia. Transl. Psychiatry 7 (11), 1264. https://doi.org/10.1038/s41398-017-0012-7.

Wu, W., Du, S., Shi, W., Liu, Y., Hu, Y., Xie, Z., Yao, X., Liu, Z., Ma, W., Xu, L., Ma, C., Zhong, Y., 2019. Inhibition of Rac1-dependent forgetting alleviates memory deficits in animal models of Alzheimer's disease. Protein & cell 10 (10), 745–759. https://doi.org/10.1007/s13238-019-0641-0.

Zang, Y., Chaudhari, K., Bashaw, G.J., 2022. Tace/ADAM17 is a bi-directional regulator of axon guidance that coordinates distinct Frazzled and Dcc receptor signaling outputs. Cell Rep. 41 (10), 111785 https://doi.org/10.1016/j.celrep.2022.111785.

Zhang, H., Ben Zablah, Y., Zhang, H., Jia, Z., 2021. Rho signaling in synaptic plasticity, memory, and brain disorders. Front. Cell Dev. Biol. 9, 729076 https://doi.org/10.3389/fcell.2021.729076.

Zhang, H., Constantine, R., Vorobiev, S., Chen, Y., Seetharaman, J., Huang, Y.J., Xiao, R., Montelione, G.T., Gerstner, C.D., Davis, M.W., Inana, G., Whitby, F.G., Jorgensen, E. M., Hill, C.P., Tong, L., Baehr, W., 2011. UNC119 is required for G protein trafficking in sensory neurons. Nat. Neurosci. 14 (7), 874–880. https://doi.org/10.1038/nn.2835.

Zhu, G., Briz, V., Seinfeld, J., Liu, Y., Bi, X., Baudry, M., 2017. Calpain-1 deletion impairs mGluR-dependent LTD and fear memory extinction. Sci. Rep. 7, 42788 https://doi.org/10.1038/srep42788.

Zhu, G., Yang, S., Xie, Z., Wan, X., 2018. Synaptic modification by L-theanine, a natural constituent in green tea, rescues the impairment of hippocampal long-term potentiation and memory in AD mice. Neuropharmacology 138, 331–340. https://doi.org/10.1016/j.neuropharm.2018.06.030.